Express Polymer Letters Vol.17, No.11 (2023) 1121–1134
Available online at www.expresspolymlett.com
https://doi.org/10.3144/expresspolymlett.2023.85

Research article

Synthesis and characteristics of α-carboxyl, ω-hydroxyl natural rubber toughened poly(lactic acid)

Abdulhakim Masa[1], *Varaporn Tanrattanakul*[2], *Ruedee Jaratrotkamjorn*[1*]

[1]Rubber Engineering and Technology Program, International College, Prince of Songkla University, 90110 Hat Yai, Songkhla, Thailand
[2]Division of Physical Science, Prince of Songkla University, 90110 Hat Yai, Songkhla, Thailand

Received 10 June 2023; accepted in revised form 24 July 2023

Abstract. This work presented the synthesis of α-carboxyl, ω-hydroxyl natural rubber (CHNR) for use as an alternative toughening agent for poly(lactic acid) (PLA). The proton nuclear magnetic resonance spectroscopy (^{1}H-NMR) and Fourier transform infrared spectroscopy (FTIR) analyses verified the chemical structure of CHNR consisting of the hydroxyl and carboxyl end groups. The molecular weights of CHNR were set from 5000 to 15 000 g·mol^{-1} which were determined by gel permeation chromatography (GPC) and ^{1}H-NMR. The PLA and CHNR were prepared by reactive blending using a twin-screw extruder. It was found that the reaction between PLA and CHNR proceeded through transesterification without a catalyst. The formation of copolymer (PLA-*co*-CHNR) at the interface of PLA and CHNR increased the interfacial adhesion between the two phases. Differential scanning calorimetry (DSC) analysis revealed that CHNR was more compatible with PLA than natural rubber (NR). The compatibilization affected the blend morphology by reducing the interfacial tension. It resulted in a reduction of rubber particle size. The CHNR with a molecular weight of 5000 g·mol^{-1} showed the greatest improvement in the toughness and ductility of PLA.

Keywords: *biopolymers, rubber, poly(lactic acid), polymer blends, copolymer, mechanical properties*

1. Introduction

Poly(lactic acid) (PLA) is an aliphatic polyester produced from renewable resources, such as sugarcane and starch. It is also known as a biodegradable and compostable polymer. It is widely used in food packaging and consumer products [1, 2]. The mechanical properties of PLA are comparable to conventional polymers, such as polystyrene (PS) and polyethylene terephthalate (PET) [3]. Therefore, it has great potential to replace conventional petroleum-based polymers because of environmental concerns and energy savings. Although PLA is environmentally friendly, biocompatible, and processable, its brittleness is a major problem that restricts its applications [2]. Several works have been studied to solve this problem. Binary blends of PLA and other polymers have successfully enhanced the toughness of PLA. It acted as a toughening agent for PLA, such as poly (polyethylene glycol-*co*-citric acid) [4], poly(β-hydroxybutyrate-*co*-β-hydroxyvalerate) [5], epoxidized polybutadiene [6], poly(styrene-*b*-butadiene-*b*-styrene) [7], poly(ethylene oxide)-poly(propylene oxide)-poly(ethylene oxide) triblock copolymers [8], poly (butylene adipate-*co*-terephthalate) [9], poly (ethylene-butylacrylate-glycidyl methacrylate) [10], poly (butylene 2,5-furandicarboxylate)-*b*-poly(ethylene glycol) [11], and poly(1,4-cyclohexanedimethylene isosorbide terephthalate) [12]. Natural rubber (NR; *cis*-1,4-polyisoprene) is an aliphatic hydrocarbon polymer that is harvested from the *Hevea brasiliensis* tree. It has several interesting properties including good mechanical properties, abrasion

*Corresponding author, e-mail: ruedee.j@psu.ac.th

resistance, and electrical insulation. It served as a good toughening agent for PLA. The toughness [13, 14] and ductility [15, 16] of PLA have been improved by blending with 10 wt% of NR. The high content of NR (>10 wt%) caused the coalescence phenomena and deteriorated the mechanical properties of the blends [13, 15]. The NR particles dispersed in the PLA matrix. It plays an important role in the mechanical properties of the blend. The craze initiates and terminates by NR particles. The compatibility of the blend is strongly associated with its mechanical properties. The difference in polarity of PLA and NR caused phase separation in the blend. It was due to the poor interfacial adhesion between the two phases. Compatibilization was a useful method to improve the compatibility of PLA and NR by adding the third component. Block and graft copolymers have been used as the compatibilizers for PLA and NR blends, such as NR-based diblock copolymer [17], NR-based triblock copolymer [18], NR grafted with poly(methyl methacrylate) [13], NR grafted with poly(vinyl acetate) [19], NR grafted with PLA [20], NR grafted with poly(butyl acrylate) [21], and NR grafted with poly(vinyl propionate) [22]. These studies were successful in improving the interfacial adhesion between the two phases and enhancing the toughness of the PLA/NR blends. These copolymers placed themselves at the interface between PLA and NR. One part was miscible with PLA and the other one was miscible with NR. Thus, the interfacial adhesion was enhanced. It allowed the stress to transform from one phase to the other one, which was efficient for craze initiation and propagation [23].

The addition of a second component with a reactive group is another approach for the compatibilization of PLA through reactive blending. If the chains of the second component are terminated by hydroxyl or carboxyl groups, three interchange reactions are possible during mixing: alcoholysis, acidolysis, and ester-ester interchange [24]. It is also known as transesterification. The block copolymer was initially formed and finally converted to the random copolymer. The blends of PLA with a second polymer through transesterification have been reported. For example, the melt blending of PLA and poly(ethylene-*co*-vinyl alcohol) through transesterification revealed a reduction of the interfacial tension and improved the interfacial adhesion between the two phases [25]. The interchange reaction between PLA and polycarbonate (PC) enhanced the compatibility of the blend and increased the interfacial adhesion between the two phases [26]. The ductility of PLA improved with the addition of maleic acid anhydride end-capped poly(propylene carbonate) [27].

The purpose of this work was to synthesize the α-carboxyl, ω-hydroxyl natural rubber (CHNR) for use as an alternative toughening agent for PLA. The blends were performed by melt mixing. We assumed that the reactive blend could proceed and generate a new copolymer. The effects of compatibilization on morphology, thermal and mechanical properties of the blends were investigated.

2. Experimental

2.1. Materials

Poly(lactic acid) (PLA Ingeo® 4043D) was produced by NatureWorks LLC, USA. The content of *d*-lactide content is approximately 6%, and a Melt Flow Index (MFI) of 6 g (10 min^{-1}) at 210 °C with a load of 2.16 kg. The melting temperature (T_m) and glass transition temperature (T_g) are approximately 145–160 and 55–60 °C, respectively. Natural rubber (NR; STR5L) with a Mooney viscosity (ML1+4 at 100 °C) of 80 was produced by Chalong Latex Industry Co., Ltd., Thailand. Periodic acid (H_5IO_6, 99%), *N*,*N*-dimethyl-4-aminopyridine (DMAP, ≥99%), and succinic anhydride (SA, ≥99%) were purchased from Sigma-Aldrich. Sodium borohydride ($NaBH_4$, 97%) was purchased from Loba Chemie Pvt. Ltd. Sodium bicarbonate ($NaHCO_3$), sodium thiosulfate pentahydrate ($Na_2S_2O_3 \cdot 5H_2O$), dichloromethane (DCM) and tetrahydrofuran (THF) were all purchased from RCI Labscan Ltd.

2.2. Synthesis of carbonyl telechelic natural rubber (CTNR)

CTNR was synthesized according to previous work [28]. NR (60 g) was dissolved in 1500 ml of THF overnight. An amount of 8.84 g of H_5IO_6 was dissolved in 97 ml of THF and added to the reactor. The reaction was carried out at room temperature for 6 h. The organic solution was filtered and washed with aqueous solutions (70/30% vol/vol of $NaHCO_3$/NaCl and 50/50% vol/vol of $Na_2S_2O_3$/NaCl). Then it dried over $MgSO_4$ and filtered through a filter paper. Finally, the organic solution was evaporated in a rotary evaporator and dried in a vacuum oven.

2.3. Synthesis of hydroxyl telechelic natural rubber (HTNR)

HTNR was synthesized according to previous work [28]. CTNR (46 g) was dissolved in 1270 ml of THF. The $NaBH_4$ (13.98 g) was added to the reactor. The reaction was carried out at 60 °C for 6 h under a nitrogen atmosphere. The organic solution was hydrolyzed with ice and washed with a saturated NaCl solution. The organic phase was dried over $MgSO_4$ and filtered. Finally, it was evaporated in a rotary evaporator and dried in a vacuum oven.

2.4. Synthesis of α-carboxyl, ω-hydroxyl natural rubber (CHNR)

HTNR (38 g) was dissolved in 1200 ml of DCM. Then the DMAP (3.19 g) and SA (7.47 g) were added to the reactor. The reaction was carried out at 30 °C for 24 h under a nitrogen atmosphere. The organic solution was washed twice with saturated $NaHCO_3$ and saturated NaCl solutions. Then it was dried over $MgSO_4$ and evaporated to remove the DCM. The obtained CHNR was dried in a vacuum oven to remove the residual DCM.

The chemical structures of all oligo-isoprenes (CTNR, HTNR, and CHNR) were verified by proton nuclear magnetic resonance spectroscopy (^{1}H-NMR) and Fourier transform infrared spectroscopy (FTIR) techniques. The molecular weights of oligo-isoprenes were determined by gel permeation chromatography (GPC) and ^{1}H-NMR.

2.5. Preparation of polymer blends

The neat PLA was dried overnight in an oven at 105 °C to remove moisture. Then it was kept in a desiccator before blending. The proportion of PLA to rubber (NR and CHNR) was fixed at 90/10 wt%. The binary blends of PLA/NR and PLA/CHNR were prepared by melt blending using a twin-screw extruder (LTE16-44, LAB TECH Engineering Co., Ltd., Thailand) at a rotor speed of 100 rpm. The temperatures of the eleven zones were set at 140 °C (feed zone), 140 °C (zone 2), 150 °C (zone 3), and 160 °C (zones 4-11). The PLA and obtained blends were shaped at 160 °C for 9 min with a pressure of 140 kg·cm^{-2} using a compression molding machine (SLLP50, Siamlab Engineering Co., Ltd., Thailand). The obtained sheet was cooled in the air at room temperature for 10 min. The thickness of the obtained sheets was approximately 2 mm.

2.6. Chemical structure analysis

The chemical structures of NR and oligo-isoprenes were verified by FTIR and ^{1}H-NMR. The FTIR spectra were recorded on the Fourier transform infrared spectrometer (Perkin-Elmer, Spotlight 200i). The absorption bands were reported in the range of 400–4000 cm^{-1} based on 16 scans at a resolution of 4 cm^{-1}. The ^{1}H-NMR data were recorded on the Varian Unity Inova NMR spectrometer (500 MHz). Deuterated chloroform ($CDCl_3$) was used as a solvent. The number-average molecular weight ($\bar{M}_n$) of all oligo-isoprenes (CTNR, HTNR, and CHNR) was determined by ^{1}H-NMR using the integrated peak areas, repeating unit of NR (68), and total mass of the rest molecule. The $\bar{M}_n$ of CTNR was calculated according to Equation (1):

$$\bar{M}_{n,CTNR} = \left[\frac{I_b}{\frac{I_{f,i}}{4}} \cdot 68\right] + 100 \quad (1)$$

where I_b and $I_{f,i}$ are the integrated peak areas at 5.10 and 2.43–2.52 ppm, respectively. 100 is the total molar mass of the rest molecule. The $\bar{M}_n$ of HTNR was calculated according to Equation (2):

$$\bar{M}_{n,HTNR} = \left[\frac{I_b}{\frac{I_e}{2}} \cdot 68\right] + 104 \quad (2)$$

where I_b and I_e are the integrated peak areas at 5.10 and 3.65 ppm, respectively. 104 is the total molar mass of the rest molecule. The $\bar{M}_n$ of CHNR was calculated according to Equation (3):

$$\bar{M}_{n,CHNR} = \left[\frac{I_b}{\frac{I_e}{2}} \cdot 68\right] + 204 \quad (3)$$

where I_b and I_e are the integrated peak areas at 5.10 and 4.08 ppm, respectively. 204 is the total molar mass of the rest molecule.

2.7. Measurement of molecular weight

The molecular weights and molecular weight distributions of PLA, NR, oligo-isoprenes, and the blends were measured by gel permeation chromatography (GPC; Agilent, 1260 Infinity II) performed with two columns (PLgel MIXED-C, 5 μm, 7.5×300 mm) and a refractive index detector. The tests were performed at 40 °C. The flow rate of eluent (THF) was 1 ml·min^{-1}. The data were calibrated with polystyrene

standards and corrected with the Benoit factor (0.67) [29].

2.8. Blend characterization

2.8.1. Mechanical properties

Izod and Charpy impact tests of PLA and the blends were carried out according to ASTM D256. Six V-notched and unnotched specimens were prepared for each test. The depth of the V-notch was 2.5 mm. The tensile properties were tested according to ASTM D412C. Six dumbbell-shaped specimens were tested using a universal testing machine (Instron 5569) at a crosshead speed of 5 mm·min^{-1}.

2.8.2. Blend morphology

The morphologies of PLA and the blends were investigated using a scanning electron microscope (FEI Quanta 400). All specimens were prepared by freeze fracturing. It was frozen in liquid nitrogen. Then the frozen specimen was rapidly fractured. The fractured surfaces were coated with gold before analysis.

2.8.3. Thermal properties

The thermal properties of PLA and the blends were investigated using differential scanning calorimetry (Perkin-Elmer, DSC7). The first heating scan was heated from –70 to 180 °C, followed by cooling from 180 to –70 °C, then heating again as in the first heating scan. The tests were performed at the heating rate of 10 °C·min^{-1} under a nitrogen atmosphere. The glass transition temperature (T_g), melting temperature (T_m), and cold crystallization temperature (T_{cc}) were determined from the second heating thermograms. The degree of crystallinity (X_c) was calculated according to Equation (4):

$$X_c\,[\%] = \frac{\Delta H_m + \Delta H_{cc}}{93} \cdot 100 \tag{4}$$

where ΔH_m and ΔH_{cc} are the enthalpies of fusion and cold crystallization in J·g^{-1}, respectively. 93 J·g^{-1} is the enthalpy of fusion of 100% PLA crystal [30].

The dynamic mechanical thermal analysis (DMA) was performed with a dynamic mechanical analyzer (DMA8000, PerkinElmer, USA). The specimens were tested in dual cantilever mode with a temperature scan from –70 to 180 °C at a heating rate of 3 °C·min^{-1}. The frequency was 1 Hz and the strain control was 0.01%.

3. Results and discussion

3.1. Characterization of oligo-isoprenes

Three types of oligo-isoprenes were synthesized from NR (Figure 1). The new oligo-isoprene (CHNR) was prepared in three steps. The first step was the synthesis of CTNR containing an aldehyde and a ketone chain ends through the controlled oxidative degradation of NR. The initial molecular weight ($\bar{M}_n$) of CTNR was set around 5000, 10 000 and 15 000 g·mol^{-1}. The CTNR was used as a starting oligo-isoprene to produce further HTNR and CHNR. A second step was the reduction of CTNR with $NaBH_4$ to generate the HTNR containing hydroxyl chain ends. The last step was the synthesis of CHNR from the HTNR by using SA in the presence of DMAP as a catalyst.

All chemical structures of the oligo-isoprenes were characterized by ^{1}H-NMR and FTIR. The ^{1}H-NMR spectra of NR and oligo-isoprenes with a targeted molecular weight of 5000 g·mol^{-1} are shown in Figure 2. NR presented the characteristic peak of CH protons at 5.10 ppm. The characteristic peaks of CTNR were observed at 9.77 and 2.13 ppm belonging to the aldehyde and ketonic protons, respectively. For the HTNR spectrum, the disappearance of the peak at 9.77 ppm was clearly observed. The presence of the new peaks at 3.80 (CH proton) and 3.65 (CH_2 protons) ppm confirmed the change of carbonyl to hydroxyl groups. The characteristic peaks of CHNR were observed at 4.08 and 2.65 ppm corresponding to the CH_2 protons adjacent to ester groups, while the peak at 3.80 ppm still appeared at the same position that was close to the hydroxyl group. These verify that the CHNR was terminated by hydroxyl and carboxyl groups.

The FTIR spectrum of NR presented the characteristic peak at 1665 cm^{-1} for the stretching vibrations of C=C (Figure 3). The CTNR presented the new absorption band at 1721 cm^{-1} corresponding to the stretching vibrations of C=O, whereas this peak

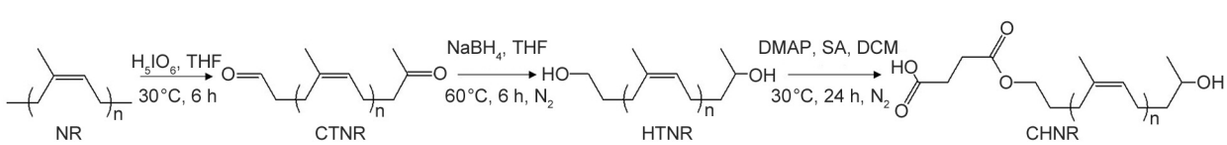

Figure 1. Synthesis of CHNR.

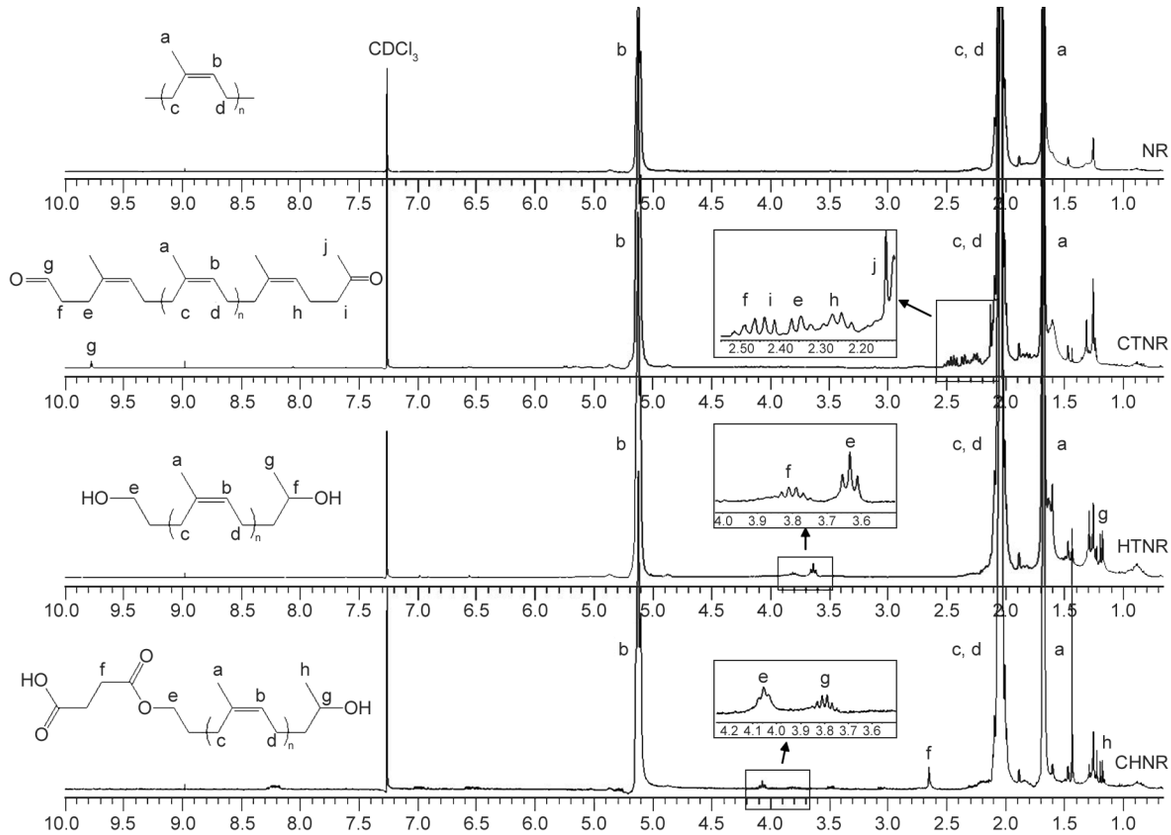

Figure 2. [1]H-NMR spectra of NR and obtained oligo-isoprenes with the targeted molecular weight of 5000 g·mol^{-1}.

disappeared after conversion to HTNR. The new absorption band of OH stretching appeared at 3378 cm^{-1}. This was due to all carbonyl groups of CTNR changing to hydroxyl groups. In the CHNR spectrum, new absorption bands were observed at 1734 and 1722 cm^{-1}. Both were assigned to the stretching vibrations of C=O in different functional groups (ester and carboxylic groups), whereas the absorption band of OH stretching at 3378 cm^{-1} still appeared. Both [1]H-NMR and FTIR data confirmed the synthesis of CHNR containing hydroxyl and carboxyl groups at the chain ends.

The molecular weights of obtained oligo-isoprenes were determined by [1]H-NMR and GPC (Table 1). It was found that the $\bar{M}_n$ of all CTNR (4466, 9018 and 14049 g·mol^{-1}) was close to the targeted molecular weights (5000, 10 000, and 15 000 g·mol^{-1}). From GPC analysis, the $\bar{M}_n$ of all CTNR were 5100, 10 100, and 14 100 g·mol^{-1}. The CTNR with initial $\bar{M}_n$ of 5000, 10 000, and 15 000 g·mol^{-1} were labeled

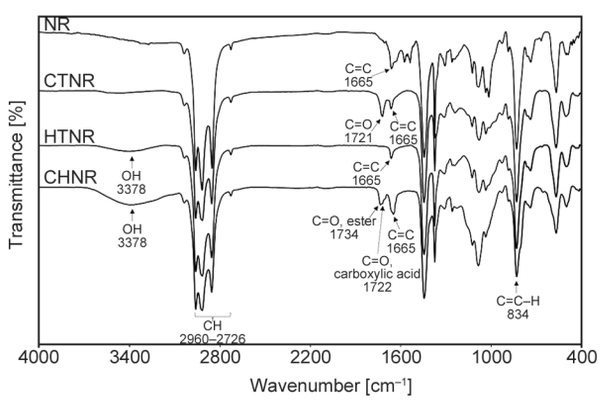

Figure 3. FTIR spectra of NR and oligo-isoprenes with the targeted molecular weight of 5000 g·mol^{-1}.

Table 1. Molecular weights of oligo-isoprenes.

Sample	$\bar{M}_n$ [g·mol^{-1}][a]	$\bar{M}_n$ [g·mol^{-1}][b]	$\bar{M}_w$ [g·mol^{-1}][b]	PDI[b]
CTNR5	4466	5100	11300	2.22
HTNR5	4746	5700	12800	2.25
CHNR5	5096	6200	12900	2.08
CTNR10	9018	10100	19700	1.95
HTNR10	9614	10600	20900	1.97
CHNR10	10747	12400	23600	1.90
CTNR15	14049	14100	36000	2.55
HTNR15	14887	15300	43900	2.87
CHNR15	15315	16600	38000	2.29

[a]Determined by [1]H-NMR.
[b]Determined by GPC.

with CTNR5, CTNR10, and CTNR15, respectively. Then they were used for the preparation of HTNR and CHNR. Both ^{1}H-NMR and GPC techniques gave a slight increase in $\bar{M}_n$ values of HTNR (HTNR5, HTNR10, and HTNR15) and CHNR (CHNR5, CHNR10, and CHNR15) from those of the CTNR because the chemical structures of their oligo-isoprenes were changed to the new ones. The polydispersity index (PDI) of all oligo-isoprenes was approximately 2.

3.2. Blend characterization

The binary blends of (PLA/NR and PLA/CHNR) were prepared by melt blending. It is known that functional groups play an important role in controlling chemical reactions. Both PLA and CHNR contained two different reactive end groups (hydroxyl and carboxyl groups). Thus, it was possible to generate new random copolymers through transesterification. The proposed mechanisms are illustrated in Figure 4. It involved three reactions: acidolysis, alcoholysis, and direct ester exchange. The block copolymer (PLA-*co*-CHNR) was initially formed in the acidolysis reaction. The PLA homopolymer and succinic acid could occur in this reaction. Succinic acid might react with PLA-*co*-CHNR, PLA, and CHNR. In this case, it acted as a chain extender that expanded the polymer chain. In the alcoholysis reaction, the formation of PLA-*co*-CHNR, PLA homopolymer, HTNR, and PLA-succinic acid might occur. HTNR could react with PLA to form the PLA-HTNR block copolymer and/or it was likely a chain extender for the polymer. The PLA-succinic acid had a chance to react with PLA, CHNR, and HTNR generating the copolymers. For direct ester exchange, the PLA-*co*-CHNR and PLA-succinic acid were formed. The block copolymers (PLA-*co*-CHNR) were initially formed and they subsequently reacted with themselves and starting

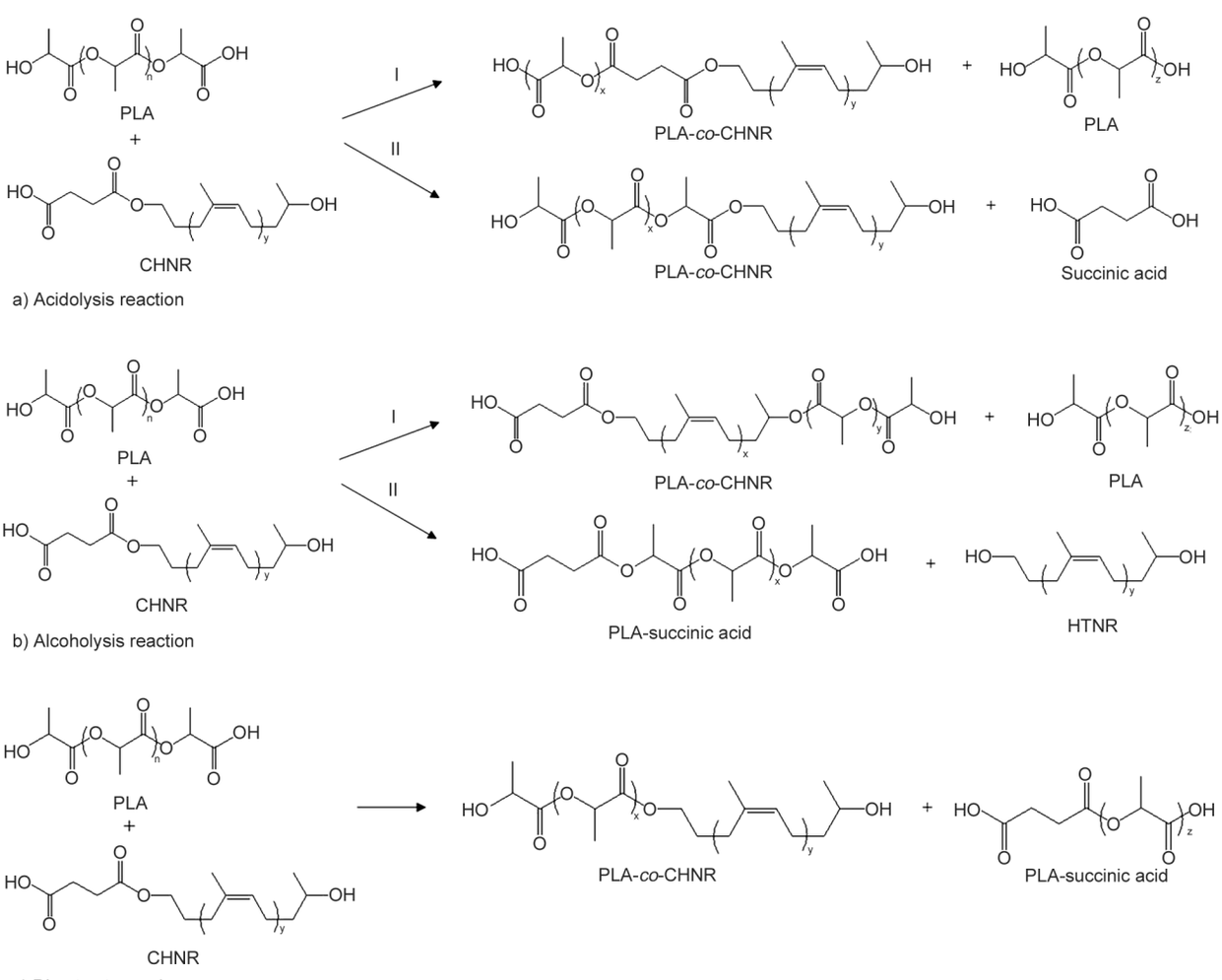

Figure 4. Transesterification reactions between PLA and CHNR. a) Acidolysis reaction, b) alcoholysis reaction, and c) direct ester exchange.

polymers (PLA and CHNR) converting to random copolymers. Based on the proposed mechanisms, it was concluded that there are different chain lengths of copolymers, homopolymers, diols, and diacids in the reaction mixture.

In fact, transesterification causes the breakage of polymer chains which leads to a decrease in the molecular weight of the polymer. In order to confirm these reactions, the measurement of molecular weight by GPC was utilized. The molecular weights and molecular weight distributions of the PLA and the blends are listed in Table 2. The $\bar{M}_n$ of PLA and NR were 81 500 and 289 000 g·mol^{-1}, respectively. The $\bar{M}_n$ of the PLA/NR was 88000 g·mol^{-1} and it increased from the $\bar{M}_n$ of PLA. This indicated that there was no chemical reaction during the melt blending. In the case of all PLA/CHNR blends, $\bar{M}_n$ had dramatically decreased from the PLA. This was due to the formation of shorter chains (new copolymers) through transesterification, as proposed in Figure 4. This is similar to a prior study on the blend between polycaprolactone and PLA through transesterification [31].

The molecular weight distribution curves of PLA, NR, and the blends are shown in Figure 5. A broad peak indicated that the molecular weight distribution of the sample was wide. In fact, polymer distributions can be wide because there are many high molecular-weight and low molecular-weight components. The PDI of the PLA/NR was approximately 2.61. Meanwhile, the PDI of PLA/CHNR was approximately 2.00. This was known as a broad distribution of polymer indicating that polymers have the distribution of chain lengths. A broad distribution of PLA/NR was due to the nature of NR. Generally, natural polymers such as NR have a width distribution. In the case of PLA/CHNR, the formation of new copolymers with different chain lengths caused the wide distribution. Thus, the GPC analysis confirmed the transesterification during the melt blending of PLA/CHNR.

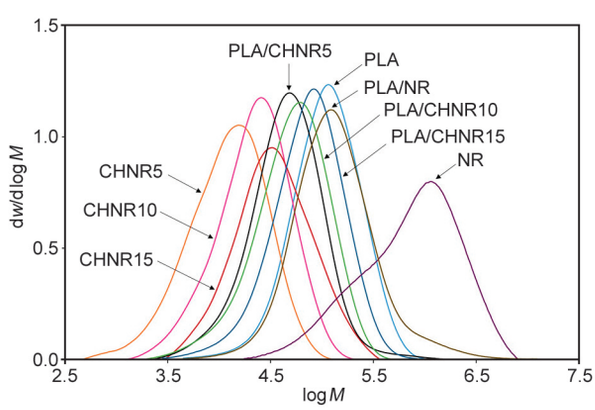

Figure 5. Molecular weight distributions of PLA and the blends.

3.3. Morphological analysis

The morphology of the blends was investigated by SEM. The SEM images of PLA and the blends at the same 500× magnification are shown in Figure 6. PLA showed fine phase morphology (Figure 6a), while phase separation was observed in the PLA/NR and PLA/CHNR blends (Figure 6b–6e). Especially, a coarse and heterogeneous morphology was clearly observed for the PLA/NR (Figure 6b). NR was dispersed in a PLA matrix. The polar PLA and non-polar NR made an immiscible blend with poor interfacial adhesion between the two phases. All PLA/CHNR blends showed a finer phase morphology than PLA/NR. Rubber particle size could indicate the compatibility in the blend. The particle size of rubber was around 10.8 μm in the PLA/NR, while the PLA/CHNR5, PLA/CHNR10, and PLA/CHNR15 were 4.2, 5.5, and 7.2 μm, respectively. The smaller particle size of the rubber indicated a reduction of the interfacial tension between the two phases [23]. It was also observed in other works [13, 19, 20, 32]. This implied that CHNR was more compatible with PLA than NR.

Table 2. Molecular weights and thermal properties of PLA and the blends.

Sample	$\bar{M}_n$ [g·mol^{-1}]	$\bar{M}_w$ [g·mol^{-1}]	PDI	T_g [°C]	T_m [°C]	T_{CC} [°C]	ΔH_m [J·g^{-1}]	ΔH_{CC} [J·g^{-1}]	X_c [%]
PLA	81 500	149 000	1.82	60	150	119	24.5	24.0	52.2
NR	289 000	1 197 000	4.14	–63	–	–	–	–	–
PLA/NR	88 000	230 000	2.61	–63, 60	150	–	6.6	6.7	14.3
PLA/CHNR5	31 000	64 300	2.07	-60, 50	141, 148	110	25.6	30.1	60.1
PLA/CHNR10	35 000	71 000	2.02	–61, 51	140, 149	101	30.9	34.8	70.6
PLA/CHNR15	49 000	98 000	2.00	–62, 52	144, 150	111	28.4	33.0	66.1

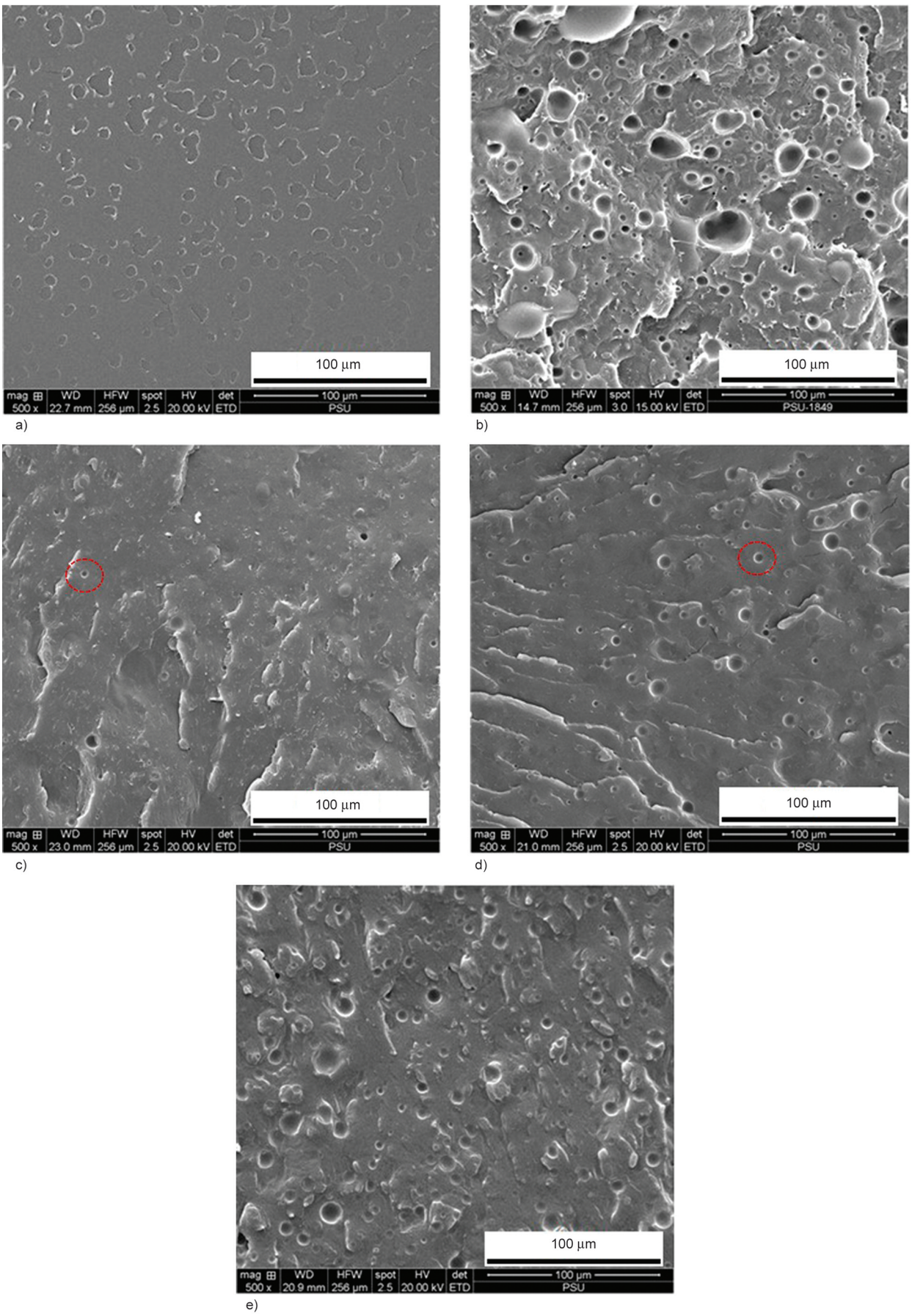

Figure 6. SEM images of PLA and the blends: a) PLA, b) PLA/NR, c) PLA/CHNR5, d) PLA/CHNR10, and e) PLA/CHNR15.

3.4. Thermal analysis

Besides the morphological analysis, the miscibility of the blend could be investigated from T_g. All thermograms were recorded during the second heating scan (Figure 7). The neat PLA and NR presented a single T_g at 60 and –63 °C, respectively. The PLA/NR exhibited two T_gs at –63 and 60 °C. The lower T_g belonged to NR, while the higher T_g belonged to PLA. The blend showed two T_gs of pure components and it was no shift from the values of their T_gs. This was a type of immiscible blend. Two T_gs and the shift of them were observed in all PLA/CHNR blends. The T_g of CHNR shifted to a higher temperature (–62–(–60 °C)), while the T_g of PLA shifted to a lower temperature (50–52 °C). It is known that a shift of T_g from one blend component towards the T_g of the other blend component is referred to as a partially miscible blend. Interestingly, the maximum shift for PLA/CHNR5 was 2 °C (T_g of CHNR) and 10 °C (T_g of PLA). It implied that CHNR5 was more compatible with PLA. Two melting peaks were notably observed for all blends, except for PLA/NR. When the sample was heated at a low rate during the temperature scan, small crystals melted and then recrystallized, resulting in the appearance of a second melting peak at a higher temperature [33]. This is a common phenomenon found in several rubbers toughened PLA [13, 16, 22, 25, 34]. The degree of crystallinity (X_c) of PLA was approximately 52.2% (Table 2). It seems that blending with NR caused a reduction in X_c of PLA to 14.3%. This was probably because the high molecular weight of NR caused more chain entanglement and hindered the nucleation of PLA. It was similarly observed in a previous study [35]. It was found that the X_c of PLA slightly increased up to 60.1–70.6% after blending with CHNR. It implied that CHNR acted as a good nucleating agent for PLA.

The mechanical and thermal properties of the material could be determined by DMA. Figure 8 shows the DMA curves of PLA and the blends. Generally, the storage modulus (E') measures the elastic response of the material. The E' (at 30 °C) of PLA decreased with the addition of NR (Figure 8a). This was due to the elastomeric nature of NR. It is known that E' is associated with the stiffness of a material. It indicated that the NR decreased the stiffness of PLA. This observation was similar to the previous report [36]. The enhancement of E' was found in the PLA/CHNR10. This can be caused by the highest crystallinity which affected the stiffness of the blend. From the DSC analysis, the X_c of the PLA/CHNR blends could be ranked in the following order: PLA/CHNR10 > PLA/CHNR15 > PLA/CHNR5. It could be concluded that the crystallinity promoted the stiffness of the blend. This behavior was similarly found in PLA blended with spent coffee grounds [37]. The E' was suddenly dropped in the temperature range of 70 to 75 °C. This is known as a glass transition region and the onset temperature is identified as a T_g. The T_g of PLA was observed at 73 °C (Figure 8b). Two T_gs were found in PLA/NR at –60 and 73 °C corresponding to the T_g of NR and PLA, respectively. The T_g of PLA in all PLA/CHNR blends was slightly shifted to the lower temperature (70–72 °C), while the T_g of CHNR was seen from –54 to –59 °C. It indicated that CHNR was more compatible with PLA than NR. All the blends showed a broad tan δ peak because the mixture had more heterogeneous polymers. The differences in the polymer

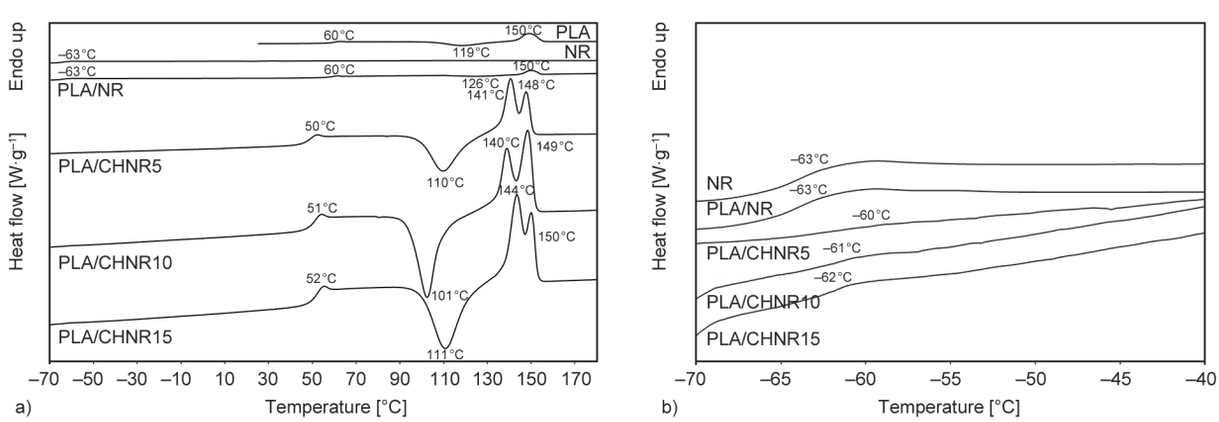

Figure 7. DSC thermograms of PLA, NR, and the blends: a) overall view, and b) expanded view for the temperature range from –70 to –40 °C.

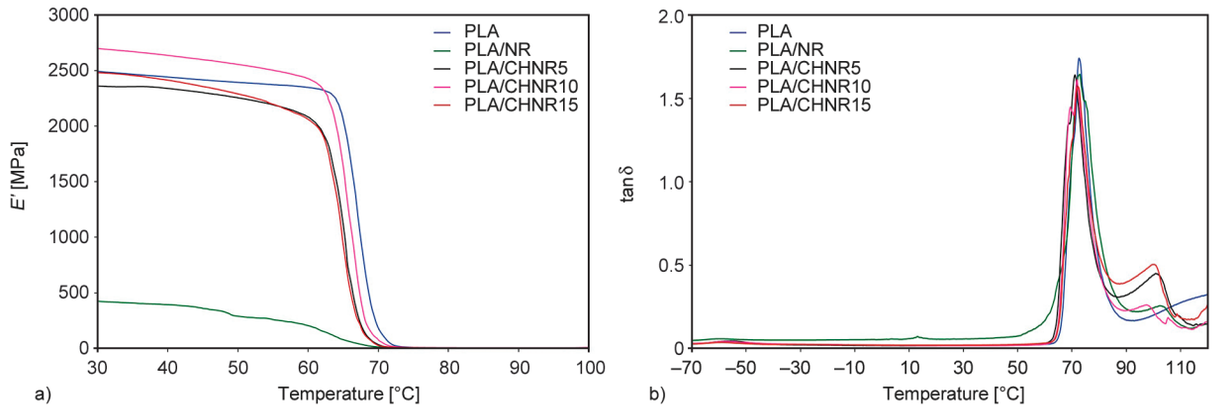

Figure 8. DMA curves of PLA and the blends: a) storage modulus and b) tan δ.

chain lengths lead to a wide distribution of relaxation times [38].

3.5. Mechanical properties

The mechanical properties of PLA and the blends are summarized in Table 3. The rubber content was 10 wt% in all blends. The impact resistance was investigated by both Izod and Charpy impact tests. Generally, the impact strength determines the toughness of a material. It measures the energy absorption during its fracture. The brittle material has lower energy absorption than ductile material. The Izod impact test differs from the Charpy impact test by the direction of the specimens in the machine. In the Izod impact test, the impact strengths of notched and unnotched PLA (2.2 and 8.2 kJ·m^{-2}) were insignificantly changed after blending with NR (3.3 and 8.7 kJ·m^{-2}). It is known that the compatibility of the blend relates to its mechanical properties. The PLA/NR was an immiscible blend that caused poor interfacial adhesion between PLA and NR phases. Therefore, it was insufficient for stress transfer between the two phases. In rubber-toughened plastic, the deformation mechanism involves shear and cavitation processes [39]. The shear processes consist of shear yielding and shear band. The cavitation processes involve crazing, voids, and fractures. The crazing and shear yielding occur simultaneously. However, crazing is currently accepted as a principal mechanism for toughening. When stress is applied to the polymer, it initiates a craze and leads to the formation of an interpenetrating network of voids. The craze initiates at a stress concentration produced by rubber particles. The craze growth propagates and terminates at rubber particles. The impact strengths of un-notched and notched specimens of PLA increased with the addition of CHNR. Interestingly, the unbroken specimens without notch of PLA/CHNR5 and PLA/CHNR10 indicated the high toughness of these blends. According to the proposed mechanism in Figure 4, the transesterification occurred at the interface of PLA and CHNR. The formation of the PLA-*co*-CHNR behaved as a bridge connecting the two phases. The stress could transfer between two phases resulting in the enhancement of impact strength. In the Charpy impact test, blending with NR slightly decreased the impact strength of un-notched PLA and insignificant changed the impact strength of notched PLA. CHNR5 and CHNR10 showed a significant enhancement in both notched and unnotched specimens. In the case of CHNR5, the impact strength increased up to 60.0 and 17.0 kJ·m^{-2}

Table 3. Impact strength and tensile properties of PLA and the blends.

Sample	Izod impact strength [kJ·m^{-2}]		Charpy impact strength [kJ·m^{-2}]		E [MPa]	σ_b [MPa]	ε_b [%]
	Unnotched	Notched	Unnotched	Notched			
PLA	8.2±0.1	2.2±0.2	18.7±0.4	2.6±0.2	1827±48	69.57±1.19	5.80±0.12
PLA/NR	8.7±0.1	3.3±0.2	15.4±0.3	3.2±0.2	1232±52	31.87±1.09	6.08±0.06
PLA/CHNR5	Unbroken	7.4±0.2	60.0±0.6	17.0±0.7	1450±64	36.88±0.35	14.52±0.11
PLA/CHNR10	Unbroken	5.1±0.1	30.1±0.3	8.7±0.6	1385±41	30.76±0.92	11.26±0.09
PLA/CHNR15	17.7±0.3	4.2±0.1	18.4±0.6	4.2±0.5	1406±53	24.81±0.96	3.04±0.04

from those of PLA at 18.7 and 2.6 kJ·m^{-2}. It seems that CHNR5 was a good toughening agent for PLA. Due to the good interfacial adhesion between the two phases, the initiation of the craze at the interface of the matrix and the dispersed phase was prevented and retarded the fracture growth. It resulted in an increase in impact strength. The chain lengths of copolymers affected their mechanical properties. The impact strength tended to decrease with molecular weight. Rubber particle size plays an important role in the mechanical properties of the blend. Larger rubber particle size promotes craze propagation, while smaller rubber particle size is insufficient to stop craze propagation and fracture. Therefore, the optimal rubber particle size could stabilize the craze growth and stop the crack. In this work, the optimal rubber particle size in PLA/CHNR blends was approximately 4–5 μm. It has been reported that the optimal rubber particle size provided the optimum mechanical properties [13, 15, 20, 22].

The tensile properties are listed in Table 3. The Young's modulus (E) and tensile strength (σ_b) of PLA dramatically decreased with the addition of NR and CHNR. Generally, the addition of soft polymers like rubber to the plastic matrix causes deterioration of E and σ_b [13, 15, 16, 20–22]. No improvement in elongation at break (ε_b) was observed for PLA/NR in comparison with the PLA. This suggests that the compatibility of the blend is strongly related to its mechanical properties. The ε_b of PLA increased significantly with the addition of CHNR5 and CHNR10, except for CHNR15. This implied that CHNR5 and CHNR10 increased the ductility of PLA. The stress-strain behaviors of PLA and the blends are shown in Figure 9. Generally, the area under the stress-strain curve correlates to the toughness of a material. The stress-strain curve of PLA showed a straight line that dropped suddenly after reaching the maximum stress point. This is a characteristic of a brittle material that has a limit absorbing the energy before failure. The stress-strain curves of PLA/CHNR5 and PLA/CHNR10 showed a larger plastic region after the yield point than PLA/NR. The large area under the curve indicates that it absorbs a large amount of energy during the plastic deformation before failure. It implied that PLA/CHNR5 and PLA/CHNR10 were more ductile materials than PLA/NR. Figure 10 presents the different types of tensile fracture surfaces. The smooth and fine fracture surface of PLA indicates a brittle fracture (Figure 10a). The immiscibility of PLA and NR caused weak interfacial adhesion between the two phases. The rubber particles were pulled away from the PLA matrix during the fracture and left the holes (Figure 10b). As a result of the absence of rubber particles, there was no prevention of craze growth. Finally, it led to the fracture of a material. The coarse surface and stress whitening were observed in all PLA/CHNR blends, which indicated the ductile fracture (Figure 10c–10e). Moreover, the presence of an optimal rubber particle size in the PLA/CHNR could retard the craze propagation and fracture. These observations supposed that the enhancement in the compatibility of the blends could improve their mechanical properties.

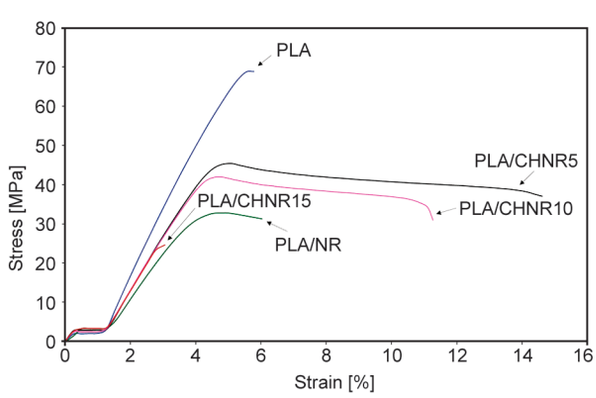

Figure 9. Stress-strain curves of PLA and the blends.

4. Conclusions

Binary blends (PLA/NR and PLA/CHNR) were prepared by melt mixing. The blend between PLA and NR was a physical blend, while the blend of PLA and CHNR was a reactive blend. The GPC analysis confirmed the formation of PLA-*co*-CHNR during blending. The compatibility of the blend is related to its mechanical properties. The CHNR was more compatible with PLA than NR. The addition of CHNR5 and CHNR10 increased the interfacial adhesion between the two phases and enhanced the impact strength and elongation at break of the PLA. The mechanical properties of the PLA/CHNR blends decreased with the molecular weight. The shorter chain length of the copolymer was more effective than the longer one. The DSC thermograms and SEM images also confirmed the compatibility of PLA and CHNR. The significant shift of T_g values in all PLA/CHNR blends implied an improvement in compatibility. The addition of CHNR did not hinder the crystallization in PLA. The optimal rubber

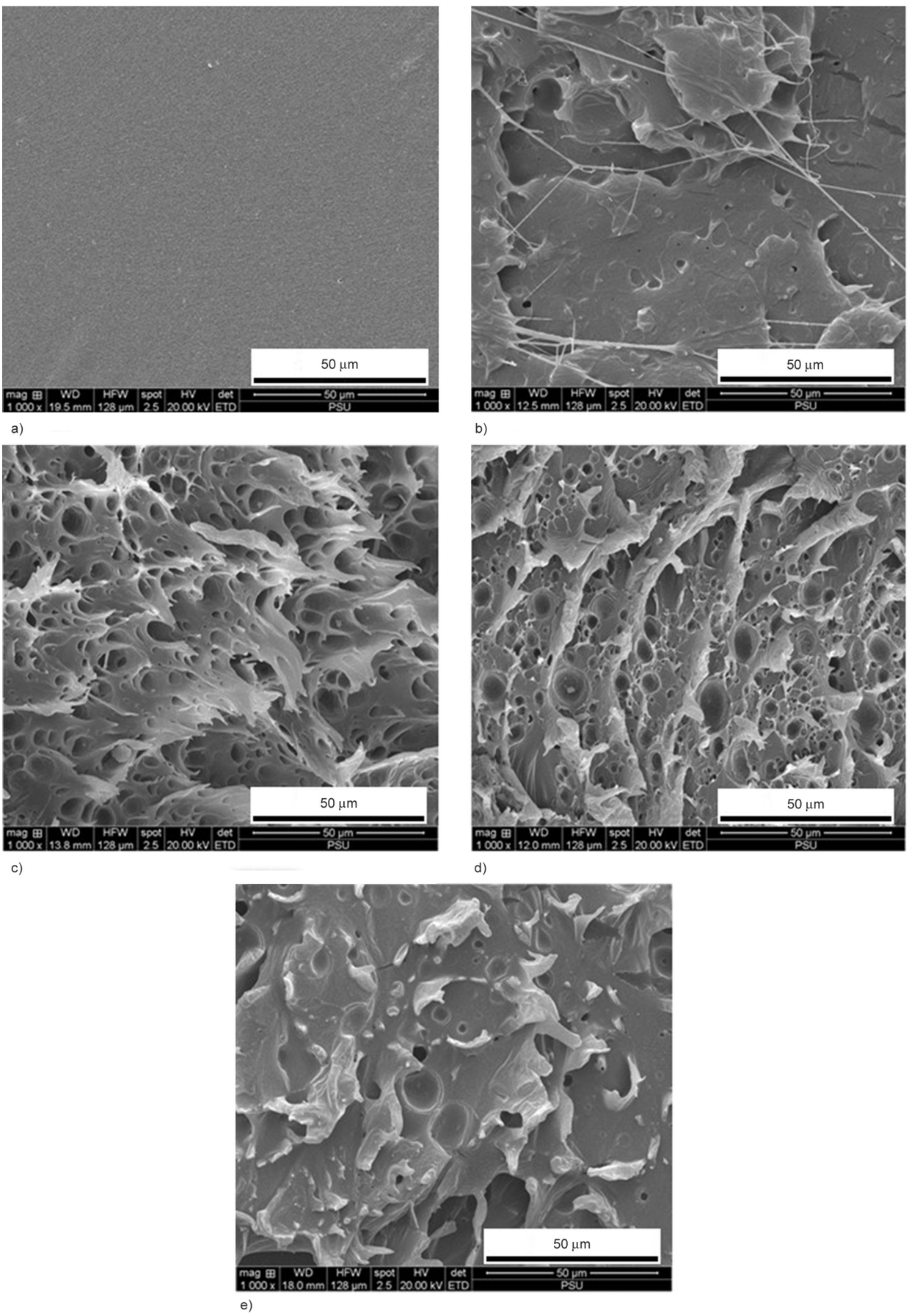

Figure 10. Tensile fracture surfaces: a) PLA, b) PLA/NR, c) PLA/CHNR5, d) PLA/CHNR10, and e) PLA/CHNR15.

particle size in the PLA/CHNR was 4.2 and 5.5 μm. It could retard the craze propagation and fracture.

Acknowledgements

This research was supported by the Prince of Songkla University (Grant No. UIC6402031S).

References

[1] Lim L-T., Auras R., Rubino M.: Processing technologies for poly(lactic acid). Progress in Polymer Science, **33**, 820–852 (2008). https://doi.org/10.1016/j.progpolymsci.2008.05.004

[2] Rasal R. M., Janorkar A. V., Hirt D. E.: Poly(lactic acid) modifications. Progress in Polymer Science, **35**, 338–356 (2010). https://doi.org/10.1016/j.progpolymsci.2009.12.003

[3] Carrasco F., Pagès P., Gámez-Pérez J., Santana O. O., Maspoch M. L.: Processing of poly(lactic acid): Characterization of chemical structure, thermal stability and mechanical properties. Polymer Degradation and Stability, **95**, 116–125 (2010). https://doi.org/10.1016/j.polymdegradstab.2009.11.045

[4] Gui Z., Xu Y., Gao Y., Lu C., Cheng S.: Novel polyethylene glycol-based polyester-toughened polylactide. Materials Letters, **71**, 63–65 (2012). https://doi.org/10.1016/j.matlet.2011.12.045

[5] Ma P., Spoelstra A. B., Schmit P., Lemstra P. J.: Toughening of poly (lactic acid) by poly(β-hydroxybutyrate-*co*-β-hydroxyvalerate) with high β-hydroxyvalerate content. European Polymer Journal, **49**, 1523–1531 (2013). https://doi.org/10.1016/j.eurpolymj.2013.01.016

[6] Wang Y., Wei Z., Leng X., Shen K., Li Y.: Highly toughened polylactide with epoxidized polybutadiene by *in-situ* reactive compatibilization. Polymer, **92**, 74–83 (2016). https://doi.org/10.1016/j.polymer.2016.03.081

[7] Wang Y., Wei Z., Li Y.: Highly toughened polylactide/epoxidized poly(styrene-*b*-butadiene-*b*-styrene) blends with excellent tensile performance. European Polymer Journal, **85**, 92–104 (2016). https://doi.org/10.1016/j.eurpolymj.2016.10.019

[8] Gu L., Nessim E. E., Li T., Macosko C. W.: Toughening poly(lactic acid) with poly(ethylene oxide)-poly(propylene oxide)-poly(ethylene oxide) triblock copolymers. Polymer, **156**, 261–269 (2018). https://doi.org/10.1016/j.polymer.2018.09.027

[9] Gigante V., Canesi I., Cinelli P., Coltelli M. B., Lazzeri A.: Rubber toughening of polylactic acid (PLA) with poly(butylene adipate-*co*-terephthalate) (PBAT): Mechanical properties, fracture mechanics and analysis of ductile-to-brittle behavior while varying temperature and test speed. European Polymer Journal, **115**, 125–137 (2019). https://doi.org/10.1016/j.eurpolymj.2019.03.015

[10] Zhao J., Pan H., Yang H., Bian J., Zhang H., Gao G., Dong L.: Study on miscibility, thermal properties, degradation behaviors, and toughening mechanism of poly(lactic acid)/poly(ethylene-butylacrylate-glycidyl methacrylate) blends. International Journal of Biological Macromolecules, **143**, 443–452 (2020). https://doi.org/10.1016/j.ijbiomac.2019.11.226

[11] Chen C., Tian Y., Li F., Hu H., Wang K., Kong Z., Ying W. B., Zhang R., Zhu J.: Toughening polylactic acid by a biobased poly(butylene 2,5-furandicarboxylate)-*b*-poly(ethylene glycol) copolymer: Balanced mechanical properties and potential biodegradability. Biomacromolecules, **22**, 374–385 (2021). https://doi.org/10.1021/acs.biomac.0c01236

[12] Park C. K., Jang D. J., Lee J. H., Kim S. H.: Toughening of polylactide by *in-situ* reactive compatibilization with an isosorbide-containing copolyester. Polymer Testing, **95**, 107136 (2021). https://doi.org/10.1016/j.polymertesting.2021.107136

[13] Jaratrotkamjorn R., Khaokong C., Tanrattanakul V.: Toughness enhancement of poly(lactic acid) by melt blending with natural rubber. Journal of Applied Polymer Science, **124**, 5027–5036 (2012). https://doi.org/10.1002/app.35617

[14] Juntuek P., Ruksakulpiwat C., Chumsamrong P., Ruksakulpiwat Y.: Effect of glycidyl methacrylate-grafted natural rubber on physical properties of polylactic acid and natural rubber blends. Journal of Applied Polymer Science, **125**, 745–754 (2012). https://doi.org/10.1002/app.36263

[15] Bitinis N., Verdejo R., Cassagnau P., Lopez-Manchado M. A.: Structure and properties of polylactide/natural rubber blends. Materials Chemistry and Physics, **129**, 823–831 (2011). https://doi.org/10.1016/j.matchemphys.2011.05.016

[16] Pongtanayut K., Thongpin C., Santawitee O.: The effect of rubber on morphology, thermal properties and mechanical properties of PLA/NR and PLA/ENR blends. Energy Procedia, **34**, 888–897 (2013). https://doi.org/10.1016/j.egypro.2013.06.826

[17] Chumeka W., Pasetto P., Pilard J-F., Tanrattanakul V.: Bio-based diblock copolymers prepared from poly(lactic acid) and natural rubber. Journal of Applied Polymer Science, **132**, 41426 (2015). https://doi.org/10.1002/app.41426

[18] Chumeka W., Pasetto P., Pilard J-F., Tanrattanakul V.: Bio-based triblock copolymers from natural rubber and poly(lactic acid): Synthesis and application in polymer blending. Polymer, **55**, 4478–4487 (2014). https://doi.org/10.1016/j.polymer.2014.06.091

[19] Chumeka W., Tanrattanakul V., Pilard J-F., Pasetto P.: Effect of poly(vinyl acetate) on mechanical properties and characteristics of poly(lactic acid)/natural rubber blends. Journal of Polymer and the Environment, **21**, 450–460 (2013). https://doi.org/10.1007/s10924-012-0531-5

[20] Sookprasert P., Hinchiranan N.: Morphology, mechanical and thermal properties of poly(lactic acid) (PLA)/natural rubber (NR) blends compatibilized by NR-graft-PLA. Journal of Materials Research, **32**, 788–800 (2017). https://doi.org/10.1557/jmr.2017.9

[21] Zhang C., Man C., Pan Y., Wang W., Jiang L., Dan Y.: Toughening of polylactide with natural rubber grafted with poly(butyl acrylate). Polymer International, **60**, 1548–1555 (2011). https://doi.org/10.1002/pi.3118

[22] Jaratrotkamjorn R., Tanrattanakul V.: Toughness improvement of poly(lactic acid) with poly(vinyl propionate)-grafted natural rubber. Journal of Applied Polymer Science, **138**, 50980 (2021). https://doi.org/10.1002/app.50980

[23] Koning C., van Duin M., Pagnoulle C., Jerome R.: Strategies for compatibilization of polymer blends. Progress in Polymer Science, **23**, 707–757 (1998). https://doi.org/10.1016/S0079-6700(97)00054-3

[24] Kotliar A. M.: Interchange reactions involving condensation polymers. Journal of Polymer Science: Macromolecular Reviews, **16**, 367–395 (1981). https://doi.org/10.1002/pol.1981.230160106

[25] Sadik T., Becquart F., Majesté J-C., Taha M.: In-melt transesterification of poly(lactic acid) and poly(ethylene-*co*-vinylalcohol). Materials Chemistry and Physics, **140**, 559–569 (2013). https://doi.org/10.1016/j.matchemphys.2013.04.004

[26] Chelghoum N., Guessoum M., Fois M., Haddaoui N.: Contribution of catalytic transesterification reactions to the compatibilization of poly(lactic acid)/polycarbonate blends: Thermal, morphological and viscoelastic characterization. Journal of Polymers and the Environment, **26**, 342–354 (2018). https://doi.org/10.1007/s10924-017-0950-4

[27] Zhou L., Zhao G., Jiang W.: Effects of catalytic transesterification and composition on the toughness of poly (lactic acid)/poly(propylene carbonate) blends. Industrial and Engineering Chemistry Research, **55**, 5565–5573 (2016). https://doi.org/10.1021/acs.iecr.6b00315

[28] Jaratrotkamjorn R., Nourry A., Pasetto P., Choppé E., Panwiriyarat W., Tanrattanakul V., Pilard J-F.: Synthesis and characterization of elastomeric, biobased, nonisocyanate polyurethane from natural rubber. Journal of Applied Polymer Science, **134**, 45427 (2017). https://doi.org/10.1002/app.45427

[29] Busnel J. P.: Data handling in g.p.c. for routine operations. Polymer, **23**, 137–141 (1982). https://doi.org/10.1016/0032-3861(82)90027-1

[30] Tsuji H., Ikada Y.: Properties and morphologies of poly(L-lactide): 1. Annealing condition effects on properties and morphologies of poly(L-lactide). Polymer, **36**, 2709–2716 (1995). https://doi.org/10.1016/0032-3861(95)93647-5

[31] Lipik V. T., Widjaja L. K., Liow S. S., Abadie M. J. M., Venkatraman S. S.: Effects of transesterification and degradation on properties and structure of polycaprolactone-polylactide copolymers. Polymer Degradation and Stability, **95**, 2596–2602 (2010). https://doi.org/10.1016%2Fj.polymdegradstab.2010.07.027

[32] Klinkajorn J., Tanrattanakul V.: Compatibilization of poly(lactic acid)/epoxidized natural rubber blend with maleic anhydride. Journal of Applied Polymer Science, **15**, 48297 (2020). https://doi.org/10.1002/app.48297

[33] Sarasua J-R., Prud'homme R. E., Wisniewski M., le Borgne A., Spassky N.: Crystallization and melting behavior of polylactides. Macromolecules, **31**, 3895–3905 (1998). https://doi.org/10.1021/ma971545p

[34] Zhang C., Wang W., Huang Y., Pan Y., Jiang L., Dan Y., Luo Y., Peng Z.: Thermal, mechanical and rheological properties of polylactide toughened by expoxidized natural rubber. Materials and Design, **45**, 198–205 (2013). https://doi.org/10.1016/j.matdes.2012.09.024

[35] Suksut B., Deeprasertkul C.: Effect of nucleating agents on physical properties of poly(lactic acid) and its blend with natural rubber. Journal of Polymers and the Environment, **19**, 288–296 (2011). https://doi.org/10.1007/s10924-010-0278-9

[36] Tessanan W., Chanthateyanonth R., Yamaguchi M., Phinyocheep P.: Improvement of mechanical and impact performance of poly(lactic acid) by renewable modified natural rubber. Journal of Cleaner Production, **276**, 123800 (2020). https://doi.org/10.1016/j.jclepro.2020.123800

[37] de Bomfim A. S. C., de Oliveira D. M., de Cavalho Benini K. C. C., Cioffi M. O. H., Voorwald H. J. C., Rodrigue D.: Effect of spent coffee grounds on the crystallinity and viscoelastic behavior of polylactic acid composites. Polymers, **15**, 2719 (2023). https://doi.org/10.3390/polym15122719

[38] Kannurpatti A. R., Anseth J. W., Bowman C. N.: A study of the evolution of mechanical properties and structural heterogeneity of polymer networks formed by photopolymerizations of multifunctional (meth)acrylates. Polymer, **39**, 2507–2513 (1998). https://doi.org/10.1016/S0032-3861(97)00585-5

[39] Bucknall C. B.: Toughened plastics. Applied Science Publishers, London (1977).